Geophys. J. Int. (2006) **165,** 763–774 doi: 10.1111/j.1365-246X.2006.02948.x

Error propagation in electromagnetic transfer functions: what role for the magnetotelluric method in detecting earthquake precursors?

O. Hanekop[1] and F. Simpson[1,2]

[1] *Geophysics Institute, University of Göttingen, Germany. E-mail: ohanekop@geo.physik.uni-goettingen.de*
[2] *Institute of Geological and Nuclear Sciences, Lower Hutt, New Zealand*

Accepted 2006 February 1. Received 2006 January 10; in original form 2004 June 2

SUMMARY

Whether electromagnetic precursors exist is a contentious issue that should be considered in the context of the focal depth and epicentral distance at which earthquakes nucleate, and with due regard to externally driven changes in the electromagnetic fields recorded at the Earth's surface. If high-frequency electromagnetic signals are generated by earthquakes, then these signals may not be detectable because of attenuation occurring between the focal depth of the earthquake and the Earth's surface. This is particularly true in seismotectonic regions (e.g. subduction zones) where saline fluids (including seawater), raised heat flow and partial melts often lead to enhanced conductivities.

A technique for examining temporal variations in magnetotelluric (MT) spectra is presented, which: (i) considers both non-inductive and inductive parts of the MT transfer function; (ii) allows electromagnetic skin depths and adjustment distances to be calculated; (iii) takes account of error propagation in the transfer functions and; and (iv) acknowledges possible non-earthquake sources of observed variations in transfer functions and their errors. Data processing tends to eliminate non-stationary electromagnetic disturbances of the source field. Hence the method is more suited to detecting hypothesized changes in subsurface conductivity than short-lived electromagnetic bursts. The technique is applied to MT data from seismotectonic regions in New Zealand (Mt. Ruapehu), the Andes (western Cordillera) and the Mediterranean (Montecristo island) and to a culturally quiet, control site situated on a stable craton in central Australia. We demonstrate that the MT method can resolve apparent conductivity changes of the order of a few percent over 48 hr time intervals and give thresholds for other interval lengths. Comparison of the results obtained from seismotectonic regions with those from central Australia, and consideration of external source field effects, highlight how temporal variations of electromagnetic fields might be speciously interpreted as earthquake precursors.

Key words: earthquake prediction, electrical conductivity, magnetotellurics.

1 INTRODUCTION

Many examples of anomalous electromagnetic signals that have been interpreted as earthquake precursors have been reported in the scientific literature. Such anomalous signals are generally manifest as increased field intensities, but they also vary considerably in frequency and other characteristics. In particular, observations that are attributed as precursors have been made in the ultra-low frequency (ULF = 0.01–1000 Hz) band (e.g. Fraser-Smith *et al.* 1990). Owing to the electromagnetic skin effect, higher-frequency signals that might arise from earthquake nucleation are likely to be attenuated to such a degree that they escape detection by sensors placed at Earth's surface (Honkura & Kuwata 1993). Attenuation of electromagnetic fields of a given frequency depends on the electrical conductivity of the subsurface—the higher the electrical conductivity, the greater the attenuation of the signal.

Electrokinetic effects (Bernabe 1998) arising from pressure-induced fluid movements (e.g. Zlotnicki & Le Mouel 1990; Yoshida *et al.* 1998) in porous rocks provide one possible source mechanism for electromagnetic precursors. A number of other effects that might explain the observed effects are discussed in Johnston (1997). Graphitization during fracture (Roberts *et al.* 1999) has been suggested as mechanism that might give rise to changes in bulk electrical conductivity and in connectivity of conductive components prior to, during and following rupture. Merzer & Klemperer (1997) and Egbert (2002) suggest that changes in the subsurface conductivity structure prior to the M7.1 Loma Prieta earthquake in California, which had a focal depth of 6 km, may have given rise to locally observed changes in ULF magnetic field amplitudes (Fraser-Smith *et al.* 1990). Unfortunately only single-component magnetic field data is available in this instance. Merzer & Klemperer (1997) estimated a change in resistivity from 30 Ωm to 0.2 Ωm in an infinite

© 2006 The Authors
Journal compilation © 2006 RAS

cylindrical body of 5–80 km^2 base area, which is situated in the fault zone. Egbert (2002) showed that even stronger changes are necessary to explain the observed magnetic field values. He presents a model where periodical changes in conductivity lead to changes in the observed magnetic field amplitudes. As the conductivity changes had to be coherent within the fault zone and match the periodicity of the observed magnetic field variations this model requires quite specific conditions, and conductivity variations of the order of 100 per cent would be required to explain the observed effects. In any case the effect should be particularly important for strong earthquakes where large fault areas are activated (Bolt 1978).

Whereas changes in electrical conductivity can be expected to be more easily detected in areas of high resistivity, seismotectonic regions are often associated with high conductivities. Despite several attempts to observe time-dependent changes in conductivity using electromagnetic measurements at the Earth's surface arising from earthquake nucleation (e.g. Park 1991; Park *et al.* 1993, and references therein) no consistent effects have been demonstrated unequivocally. Long-term changes in fault zone conductivities have been observed (e.g. Madden *et al.* 1993) but could not unambiguously be related to tectonic processes. Changes in the conductivity structure within active volcanoes have been reported (Sasai *et al.* 2002; Zlotnicki *et al.* 2003), but these have been attributed to major structural changes rather than to stress- or pressure-induced variations. However, correlations between stress-induced changes in conductivity and changing water levels in reservoirs have been reported (Hautot 2005).

The most commonly employed techniques for identifying earthquake precursors involve the visual inspection of electric (e.g. Sasai *et al.* 2002) or magnetic field time-series or of power spectra (e.g. Fraser-Smith *et al.* 1990; Molchanov *et al.* 1992; Hayakawa *et al.* 1996) for the presence of anomalous signals. These rudimentary approaches have the following limitations:

(i) lack of a systematic method for precluding as earthquake precursors temporal variations in the electromagnetic time-series arising from processes external to the Earth (i.e. perturbations in the external source field);

(ii) lack of a convincing model that explains the propagation of high-frequency electromagnetic signals from the hypocentre to electromagnetic sensors located at the Earth's surface; and

(iii) lack of confidence intervals reduces the objectivity of such analyses.

The external geomagnetic field provides time-varying signals of strongly variable amplitudes spanning a wide frequency range. These electromagnetic fluctuations induce electric currents in the Earth, which produce secondary electromagnetic fields that can be utilized as a source for probing the electrical conductivity structure of the Earth to depths of ∼600 km depth using the magnetotelluric (MT) technique. However, for the purpose of detecting electromagnetic precursors arising from earthquakes, the time-varying external electromagnetic source field constitutes a source of background noise. Other internal sources of noise include sensor noise, seismic vibrations and extraneous man-made currents. Anomalous signals generated by such background noise may be misinterpreted as earthquake precursors by the unwary and unsceptical. Obviating such misinterpretations is a necessary task if false alarms are to be avoided.

In this paper we use MT data to investigate the limits on the temporal resolution of subsurface conductivity changes. Temporal variations in both inductive and non-inductive parts of MT transfer functions derived from short, sequential data segments recorded in New Zealand (Mt. Ruapehu), the Andes (Bolivian Antiplano) and the Mediterranean (Montecristo island) are considered in the context of their confidence intervals. The results of the analysis are compared with similarly derived MT transfer functions from a control site located on a tectonically stable craton in Australia. All of the data sets were recorded using Göttingen RAP data loggers (Steveling & Leven 1992), three-component, Magson, fluxgate magnetometers and Ag-AgCl electrodes.

2 THE MAGNETOTELLURIC METHOD

The MT technique (Cagniard 1953) is a passive electromagnetic depth sounding technique that uses the electromagnetic fields induced in the Earth by variations in the external geomagnetic field to estimate a frequency-dependent impedance tensor, $\underline{\underline{Z}}$, between two orthogonal (in this paper always magnetic north–south [x] and east–west [y]) components of the electric $\underline{\mathrm{E}}$ and magnetic $\underline{\mathrm{H}}$ fields:

$$\begin{pmatrix} E_x(\omega) \\ E_y(\omega) \end{pmatrix} = \begin{pmatrix} Z_{xx}(\omega) & Z_{xy}(\omega) \\ Z_{yx}(\omega) & Z_{yy}(\omega) \end{pmatrix} \begin{pmatrix} H_x(\omega) \\ H_y(\omega) \end{pmatrix}. \tag{1}$$

Apparent resistivities $\rho_{a_{i,j}}$ can be calculated from

$$\rho_{a_{i,j}}(\omega) = \frac{1}{\omega\mu_0} |Z_{i,j}(\omega)|^2. \tag{2}$$

and impedance phases are given by

$$\varphi_{i,j} = \tan^{-1}\left(\frac{Im[Z_{i,j}(\omega)]}{Re[Z_{i,j}(\omega)]}\right). \tag{3}$$

Because the propagation of electromagnetic fields within the Earth is diffusive, MT transfer functions represent volume averages rather than point soundings of electrical conductivity. As such, small-scale changes in conductivity structure at depth may produce perturbations that are too insignificant to be resolved by electromagnetic measurements at the surface. In contrast, significant non-inductive (galvanic) effects may be produced by conductivity anomalies having dimensions smaller than the penetration depth of a particular electromagnetic sounding period. Galvanic effects arise from charges at boundaries of multidimensional bodies, are real valued and, therefore, frequency independent. Hence the impedance tensor can be decomposed into two matrices: one with real-valued components that represents galvanic effects, the other with complex components, which represent inductive effects (Bahr 1988). For example, given data aligned in the (x', y') coordinate system of a regional 2-D structure, the impedance tensor can then be expanded as:

$$\begin{aligned} \underline{\underline{AZ}}_{2D} &= \begin{pmatrix} a_{11} & a_{12} \\ a_{21} & a_{22} \end{pmatrix} \begin{pmatrix} 0 & Z_{x'y'} \\ Z_{y'x'} & 0 \end{pmatrix} \\ &= \begin{pmatrix} a_{12}Z_{y'x'} & a_{11}Z_{x'y'} \\ a_{22}Z_{y'x'} & a_{21}Z_{x'y'} \end{pmatrix} = \underline{\underline{Z}}. \end{aligned} \tag{4}$$

Within each column of $\underline{\underline{Z}}$ in (4) only one phase occurs because the assumption of galvanic distortion requires that the elements of the distortion matrix, $\underline{\underline{A}}$, must be real and frequency independent. Eq. (4) describes a scenario in which (unlike for the simple 2-D induction case) one magnetic field component and the electric field component correlated with it are not necessarily orthogonal. In the coordinate system of the electromagnetic strike, the angular deviations, β_1 and β_2, from orthogonality between coupled electric and

© 2006 The Authors, *GJI*, **165,** 763–774
Journal compilation © 2006 RAS

magnetic fields, or skew angle, is given by:

$$\tan(\beta_1) = \frac{Z_{xx}}{Z_{yx}} = -\frac{a_{12} Z_{y'x'}}{a_{22} Z_{y'x'}}. \quad (5a)$$

$$\tan(\beta_2) = \frac{Z_{xy}}{Z_{yy}} = \frac{a_{21} Z_{x'y'}}{a_{11} Z_{x'y'}}. \quad (5b)$$

Recent work on the connection between distortion of electric fields and percolation phenomena in the crust (Bahr 2000) has provided evidence that a particular type of distortion is associated with conductive networks in the vicinity of the percolation threshold. Minor changes in stress in a rock close to the percolation threshold may lead to opening or closing of interconnected fluid-bearing channels (Gueguen *et al.* 1991), thus effecting bulk conductivity. Whether resolvable temporal variations in the distortion parameters occur is an open question that will be investigated in this paper by testing whether significant temporal variations are exhibited by the skew angles given by eqs (5a) and (5b).

The sum squared (ssq) of the impedance tensor, which contains the information provided by all four impedance tensor elements and is rotationally invariant (Szarka & Menvielle 1997) will also be considered, as it provides a robust measure of impedance tensor magnitudes. The ssq function is defined by

$$ssq(\mathrm{Re}[Z]) = \mathrm{Re}^2[Z_{xx}] + \mathrm{Re}^2[Z_{xy}] + \mathrm{Re}^2[Z_{yx}] + \mathrm{Re}^2[Z_{yy}]$$
$$ssq(\mathrm{Im}[Z]) = \mathrm{Im}^2[Z_{xx}] + \mathrm{Im}^2[Z_{xy}] + \mathrm{Im}^2[Z_{yx}] + \mathrm{Im}^2[Z_{yy}]. \quad (6)$$

The error σ_f of a parameter $f(x_1, x_2, \ldots)$ is

$$\sigma_f = \sqrt{\sum_i \left(\frac{\partial f}{\partial x_i}\sigma_{x_i}\right)^2}, \quad (7)$$

where σ_{x_i} is the error of the variable x_i. The bivariate coherence is defined by:

$$r_i = \left(Z_{ix}\langle H_x E_i^*\rangle + Z_{iy}\langle H_y E_i^*\rangle\right) / \langle E_i E_i^*\rangle \qquad i = x, y, \quad (8)$$

where Z_{ij} are the estimated transfer functions and $\langle \ldots \rangle$ represents stacked cross-spectra.

When applying the MT technique, we assume that at mid-latitudes (far from the complicated current systems generated by the equatorial and auroral electrojets), large-scale, uniform, horizontal sheets of current in the distant ionosphere give rise to plane waves at the surface of conductive earth. Non-planar source excitations constitute a source of external noise that may give rise to time-variant perturbations of the MT impedance tensor if signal-to-noise ratios are inadequate. When MT is used for probing the conductivity structure of the Earth, the effects of such noise can generally be obviated by choosing sufficiently long data-recording times for the sounding period of interest, an appropriate processing technique and stacking the transfer functions (or spectra) obtained from a large number of estimates (see e.g. Simpson & Bahr 2005). However, the quest for electromagnetic precursors presents more demanding problems than standard conductivity sounding in these respects:

(i) down-weighting of events exhibiting temporal variations in the external source fields may also filter any anomalous signals arising from changes internal to the Earth;

(ii) investigating temporal electromagnetic field variations necessarily limits the length of individual time-series windows that are analysed to timescales on which we might expect the sought after precursors to occur;

(iii) stacking improves the confidence intervals of estimates, but such a method of averaging will also smooth out any temporal variations that are produced in the Earth.

We can, therefore, expect the confidence intervals associated with MT transfer functions to be larger when electromagnetic precursors rather than the electrical conductivity of the Earth are the subject under investigation. (For the sounding periods considered in this paper, 68 per cent confidence intervals for the MT transfer functions of less than 1 per cent can be achieved in the latter case if modern instrumentation and processing techniques are employed (e.g. Simpson 2001).)

3 THE EFFECT OF SUBSURFACE RESISTIVITY CHANGES ON MAGNETOTELLURIC TRANSFER FUNCTIONS

In order to estimate the effect of a hypothetical earthquake related conductivity change in parts of the subsurface we calculated 2-D and 3-D forward models of a fault zone, choosing as our example a simplified version of the San Andreas fault near Parkfield (Unsworth & Bedrosian 2004). The model consists of a fault zone conductor (FZC) of 3 Ωm and different resistivities to the sides (Fig. 1). In order to model the effect of shallow earthquakes, the resistivity in the lower 800 m of the FZC resistivity was varied from 1 to 9 Ωm. Fig. 2(a) shows the resulting change in apparent resistivities (ρ_a) as function of FZC resistivity and period at site 1, about 5 km from the FZC and site 2 directly above the FZC (Fig. 1). Variations in ρ_a of more than 30 per cent can be observed above the FZC for strong resistivity changes, whereas changes of only 15 per cent were found 5 km from the FZC. Assuming a resolution of the MT method of 5 per cent for short time intervals, only resistivity changes in the modified portion of the FZC of $\geq$15 per cent will be resolvable at sites lying above the FZC, while changes of the order of 100 per cent are needed to create a resolvable resistivity change at a site 5 km from the FZC.

In a second model, the FZC was extended by 400 m in depth, for example, representing the opening of fissures during an earthquake that are filled with conductive fluids present in the FZC (Fig. 2b). The resistivity of the extension of the FZC was varied between 3 and 27 Ωm. As the effected volume is only half of that of the previous

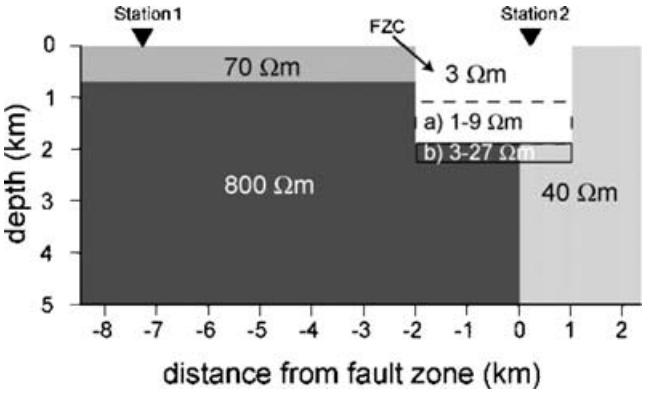

Figure 1. Simplified resistivity model of the San Andreas Fault near Parkfield (Unsworth & Bedrosian 2004). In order to test the variation of the MT apparent resistivity when conductivity changes in the fault zone occur model studies with (a) resistivities of 1–9 Ωm in the lower 800 m of the fault zone conductor (FZC) and (b) a 400-m-depth extension of the FZC with resistivities from 3–27 Ωm were performed. The results are shown in Fig. 2.

© 2006 The Authors, *GJI*, **165,** 763–774
Journal compilation © 2006 RAS

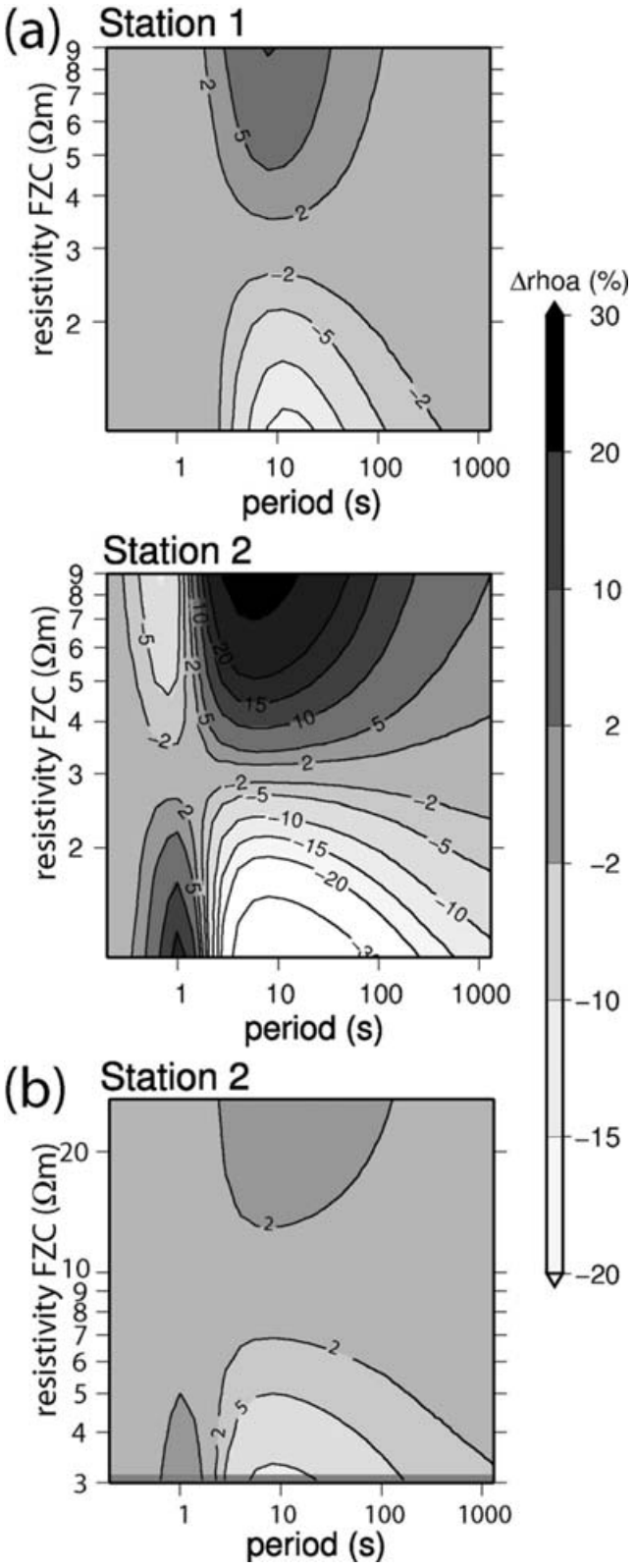

Figure 2. Deviations in apparent resistivity in the strike direction of the fault zone as function of sounding period and FZC resistivity for the model in Fig. 2. The deviations are plotted in percent from the values calculated for a FZC as shown in Fig. 1 (with 3 Ωm, 2 km deep). (a) Deviations for resistivity variations in the lower 800 m of the FZC. (b) Results for a FZC that is extended by 400 m with resistivities between 3 and 27 Ωm.

model the changes in ρ_a are only up to 10 per cent for resistivities of 3 Ωm in the lower FZC. The effect diminishes with distance from the fault zone, reaching the assumed observation resolution of 5 per cent at a distance of about 5 km.

In order to test if a limited extent of the resistivity change along the fault affects the results, we calculated the same models as in Fig. 1 with Mackie & Booker's (1999) 3-D forward modelling code and a limited extent along the fault zone. For an effected fault length of more than twice the fault width we observed only minor differences between the 2-D and 3-D models.

4 ERROR ESTIMATION AND TEMPORAL STABILITY OF MT TRANSFER FUNCTIONS

In order to investigate the temporal stability of MT transfer functions and their confidence intervals in the absence of earthquake activity, we examined high-quality MT data from a site near Mt. Doreen (DOR) in the Tanami desert, central Australia (Simpson 2001). The site lies on a stable craton at geomagnetic mid latitude, far from plate boundaries, coastlines and artificial sources of electromagnetic noise. For the purpose of the analysis, the data, which were recorded over a 3 month time interval in 2000, were divided into intervals of 48 hr and each interval was processed individually. Three different MT processing schemes were applied to the data: a robust single-site processing scheme (SS), a remote-reference (RR, Gamble *et al.* 1979) processing scheme (recent version of the code described by Egbert & Booker 1986) and Egbert's (1997) multi-site (MS) scheme. Whereas remote reference uses magnetic data recorded at a single distant site to remove uncorrelated noise from MT data MS processing combines magnetic field data from a number of sites to reduce the noise level and identify possible correlated noise in the data.

Normalized apparent resistivities, impedance phases and ssq values at periods of 57 s and 315 s are plotted for sequential 48 hr intervals in Fig. 3. MT transfer functions obtained from processing of the whole available data set were used as normal values. These transfer functions have confidence intervals less than 1 per cent. The normalization was performed to accentuate deviations of the transfer functions from their expected values, since it is these deviations rather than absolute values in which we are interested.

If the confidence intervals are adequately estimated then the variance of the transfer functions calculated from independent data segments should lie within the calculated confidence intervals. However if the plane wave assumption used in the MT method is violated this will not be reflected in the error bars, which reflect only measurement errors and not violations in the assumptions of the chosen method. Fig. 3(a) shows that variations in apparent resistivity estimated from SS processing are significantly larger than the calculated 68 per cent confidence intervals at both periods. For a number of intervals a clear trend is apparent (e.g. around days 26–34) while for 57 s the SS processing results are in general lower than the mean values. The same can be seen in the sqq values and to a lesser extent in the impedance phases. Application of RR or MS processing tends to remove this effect . The reference sites (ULU, WRA and VIC; Simpson 2001) all lie between 300 and 450 km from DOR and from each other. Examination of the magnetic field intensities (Fig. 3f) shows that the greatest deviations from the mean values derived from the SS processing occur when the amplitudes of the external magnetic field are low. Low source-field amplitudes lead to decreased signal-to-noise ratios (indicated by low coherences in

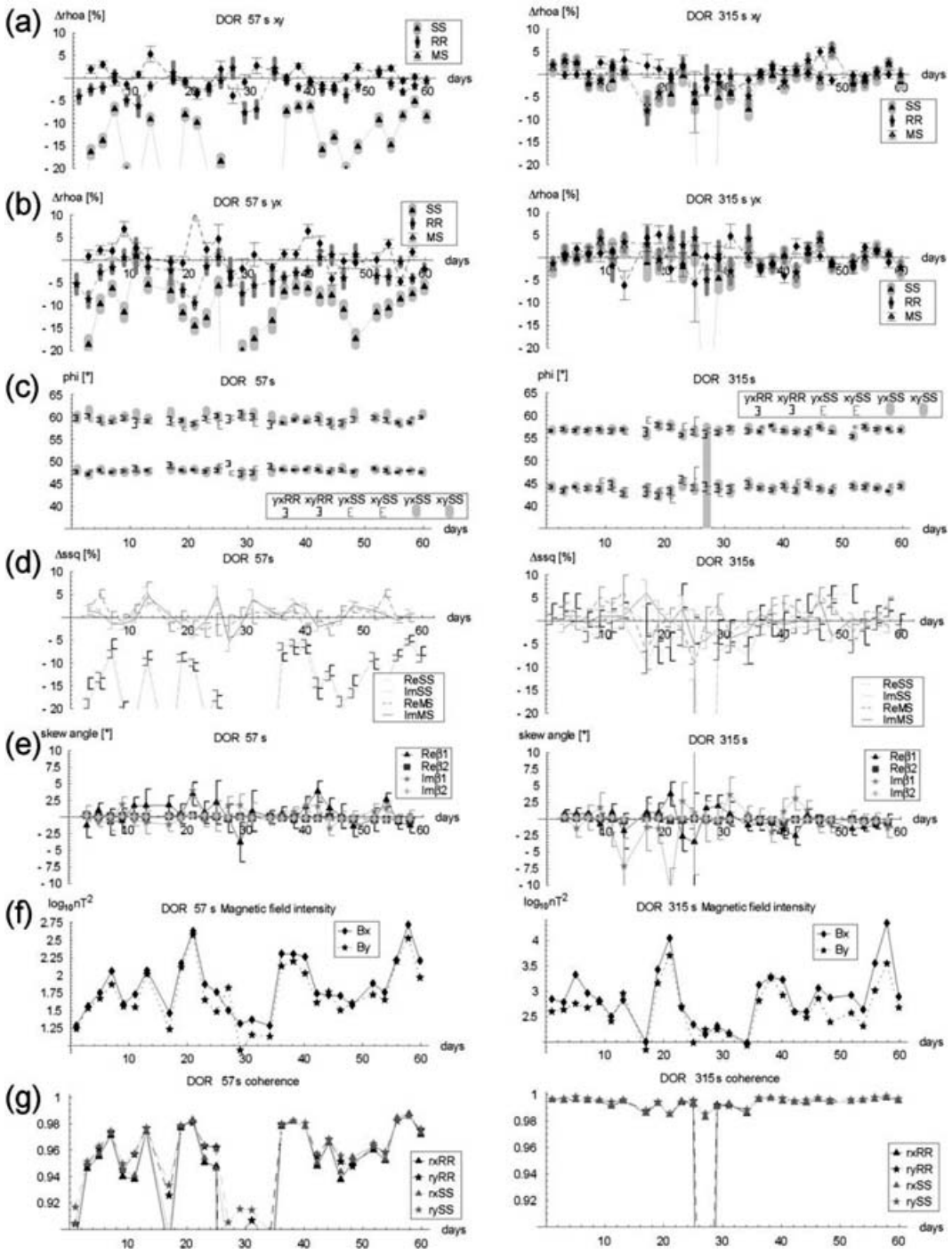

Figure 3. Temporal behaviour and 68 per cent confidence intervals for (a) apparent resistivities (N–S) (b) apparent resistivities (E–W direction) (c) impedance phases (d) ssq values (e) skew angles (f) magnetic field intensities (magnetic north, B_x, and magnetic east, B_y, power spectra) and (g) coherence derived from an MT station near Mt. Doreen (DOR) in central Australia (Simpson 2001). Each data point represents a 48-hr-processing interval. Results from single site (SS), remote reference (RR) and multisite (MS) processing are shown.

Fig. 3g), and temporal down-biasing of the impedance amplitudes (and hence apparent resistivities) during intervals of low magnetic activity and can thus be understood to be caused by noise in the magnetic fields in the manner described by Sims *et al.* (1971). The biasing effect is less obvious in the impedance phases, because they are calculated from the ratio of two biased values (eq. 3), and is also more effectively negated when the influence of local magnetic noise on the transfer function is reduced by applying RR or MS technique. The most likely source of this type of noise is the flux-gate magnetometer.

Although RR and MS processing are effective at reducing the effects of sensor noise, the transfer functions obtained from both processing techniques nevertheless show variations that are larger than predicted by their 68 per cent confidence intervals. Given that no internal changes in conductivity structure are expected in this stable tectonic region, these variations most likely arise from violations of

© 2006 The Authors, *GJI*, **165,** 763–774
Journal compilation © 2006 RAS

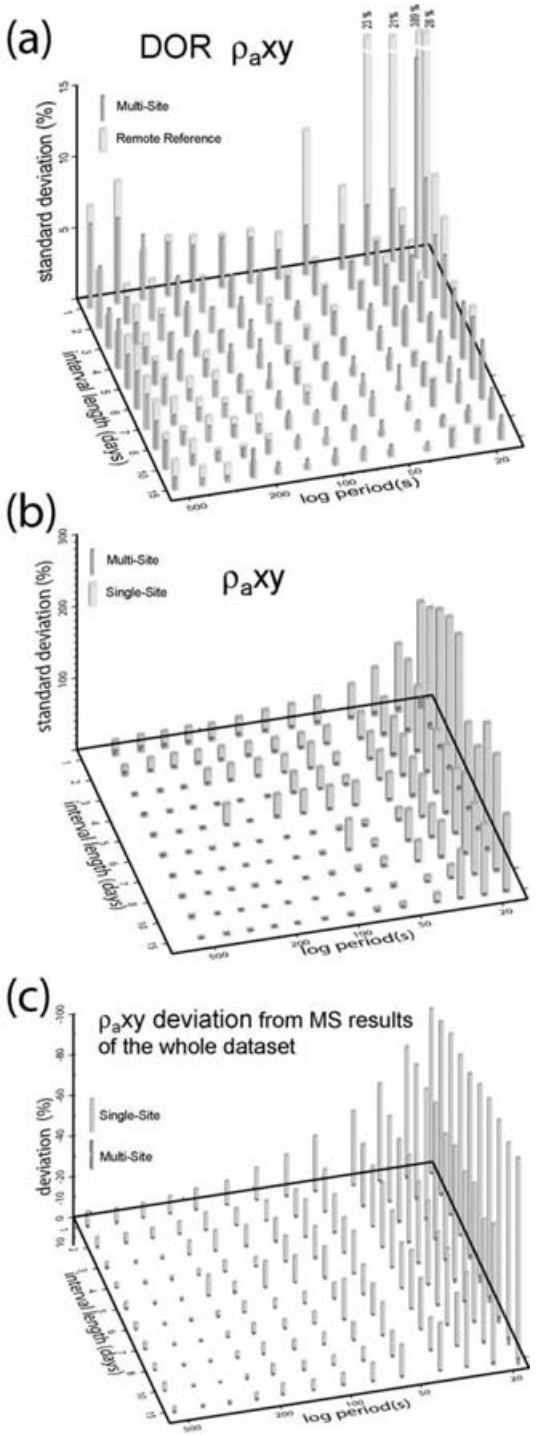

Figure 4. Standard deviation of the apparent resistivities (*xy*) for different interval length and periods (a) for RR and MS and (b) SS and MS processing calculated from the single interval results. Deviations are plotted in percent of the mean value of all intervals for one interval length and period. (c) Deviation of SS and MS weighted mean values for different interval length and periods in percent of the MS results of the whole data set.

the plane-wave assumption (PWA). Violations of the PWA, which could arise from Pc3 pulsations (Egbert *et al.* 2000) lead to low coherence between electric and magnetic field spectra (Fig. 3g). As the coherence is used to estimate the error bars violations of the PWA lead to larger errors but not necessarily to down-biased transfer functions as in case of noise. Such events would normally not be stacked when computing a standard MT transfer function for the purpose of probing the interior of the Earth.

Maximum variations between the 48 hr intervals are 5 per cent for the apparent resistivities and 3° for the phases (Fig. 3). These variations are of the same order of magnitude as variations observed by Eisel & Egbert (2001), who studied data from 24 hr intervals. In order to investigate the influence of the interval length on the stability of the transfer functions we divided the whole data set in non-overlapping intervals of 1–15 days. Standard deviations of the apparent resistivities were calculated for each interval length. Comparisons of the apparent resistivity standard deviations for a range of frequencies and interval length obtained from MS and RR processing are plotted in Fig. 4(a) (*xy* component) and those obtained from MS and SS processing in Fig. 4(b). In both cases the standard deviation is plotted in percent of the apparent resistivity of the mean value for each interval length. Similar standard deviations of the apparent resistivities estimated from the different intervals with RR and MS processing indicates that the RR processing technique is already adequate for dealing with the low-noise conditions in central Australia. Only for short periods does the MS processing appear to be more effective in removing the above mentioned effect of low signal to noise ratios. Both processing schemes lead to large standard deviations for short periods and short time intervals. The most stable results are obtained in a frequency range between 50–300 s. This is related to the fact that for long periods the amount of data limits the resolution, while lower geomagnetic field amplitudes and sensor sensitivities lead to larger variations for short periods. For SS processing, however, the standard deviations are significantly larger, in particular for short time intervals (Fig. 4b). In this case even long interval lengths (i.e. larger amounts of data) do not lead to more stable results for short periods. As the standard deviation for both RR and MS processing are orders smaller than for SS processing this gives additional weight to the hypothesis of local noise as the source of low temporal stability of the transfer functions.

Fig. 4(c) plots the percentile deviation of the weighted mean of the apparent resistivities (MS and SS processing) from the MS results for the whole data set. Whereas the weighted MS results show small deviations from the reference, the SS results for short periods are significantly down-biased (note inverted *z*-axes in Fig. 4c). Even for the longest time intervals of 15 days, the down-bias at 40 s is more than 25 per cent. This indicates the necessity of using RR or MS processing to obtain reliable apparent resistivity results at short periods. As noted above, phase values are significantly more stable for all frequencies, interval length and processing schemes. The standard deviations of the phases for RR and MS processing show a similar period and interval length behaviour as those of the apparent resistivities in Fig. 4(a) but with about half the amplitudes (not plotted).

As the variations in amplitude and error levels increase dramatically when shorter time intervals are used to calculate the MT transfer functions, 24 hr intervals can be regarded as the limit for the temporal resolution of MT data at periods around 100 s unless overlapping time intervals are used. In addition to external geomagnetic field variations, the choice of processing technique and instrumentation, the level of cultural noise present in the recording region will also impose limitations on the resolution of temporal variations arising from conductivity changes in the Earth. In every regard, it would be difficult to find a recording site on our densely populated planet that is more devoid of cultural noise than our chosen control site, which we consider to be ideally located.

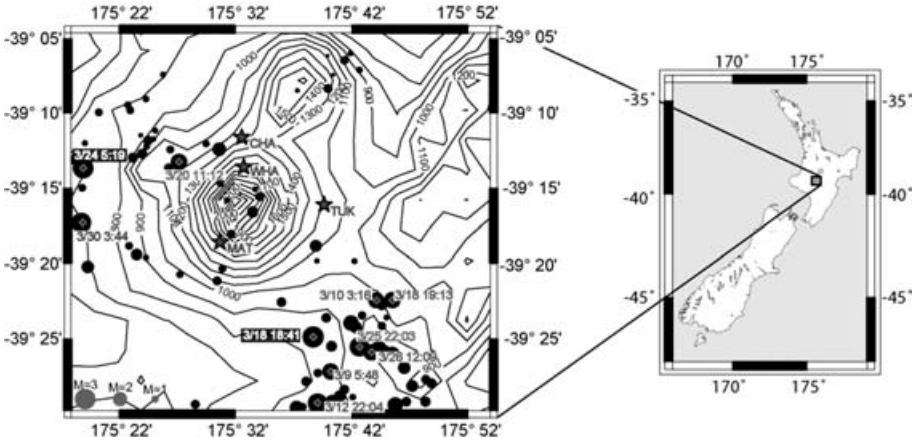

Figure 5. Topographic map of the region around Mt. Ruapehu, New Zealand. Stars indicate the positions of the MT sites. The black circles indicate the epicentres and magnitudes of earthquakes that occurred during the 6 week MT recording interval. Occurrence times are shown for the 10 largest earthquakes. (Earthquake data from www.geonet.org.nz).

5 INVESTIGATIONS IN SEISMICALLY ACTIVE REGIONS

Mt. Ruapehu, New Zealand

Mt. Ruapehu is one of New Zealand's most active volcanoes. It has erupted more than 50 times in the last 150 yr. The last major eruption was in 1995–1996 (Gamble *et al.* 1999) and an intense volcanic tremor occurred on 17th July 2000. Today small volcanic tremors are common.

Mt. Ruapehu is centrally located on the North Island of New Zealand (Fig. 5), and defines the southern end of the seismically and geothermally active Taupo Volcanic Zone. Four long-period MT stations were installed on the flanks of the volcano for a 6 week interval from 2002 February 22 to 2002 March 29. During this time a number of small earthquakes occurred in the region. Most of these earthquakes had magnitudes of ∼3 and focal depths of 10–15 km. Their epicentres and the site names and locations of the MT instruments are shown in Fig. 5.

In order to investigate possible earthquake-related effects in the MT transfer functions, data from site WHA was analysed in 48 hr intervals in a similar way to the approach employed for DOR (the control site in central Australia), with magnetic field data from site TUK being used for RR processing. As only two sites had sufficiently long recording times no MS processing was possible in this case. Here we assume that there should be some degree of correlation between any earthquake precursors detected at the two sites on the volcano, if this is not so than remote reference processing will eliminate earthquake precursors in the same way as other forms of non-stationary disturbance. Structural investigations of the MT data showed resistivities of 50–100 Ωm for the upper 20 km below Mt. Ruapehu. Therefore, we investigate variations with a period of 57 s which are most sensitive at the epicentral depth and distances of reported earthquakes. Figs 6(a)–(c) show the magnetic field power spectra and temporal variations in the apparent resistivity for 48 hr intervals. As for the case of the Australian control site, the strongest perturbations in the apparent resistivity (Fig. 6a) occur during times of low external field intensities and low coherences (Figs 6b and c).

In order to investigate possible short-lived temporal changes in the apparent resistivities results for 24 hr intervals were also calculated. The results are shown in Figs 6(d)–(f). In general similar results to those for the longer intervals are obtained. Increasing the length of the time windows analysed by a factor two results in a factor of ∼2 larger variations and errors in the apparent resistivity. From March 19th onwards the magnetic field intensities and coherences for the 24 hr intervals show a quite erratic pattern that coincides with the occurrence of the two largest earthquakes during the measurements. Comparison of the magnetic field intensities at site WHA (Fig. 6e) with the k_p-index (Rangarajan 1989) indicates disturbed geomagnetic activity during late March 2002 with sudden commencements of magnetic storms reported for March 18th and 20th, which are clearly visible in the measured time-series. Comparison between the magnetic field data at our field sites with data from the magnetic observatory in Eyrewell (NZ, South Island, about 450 km southwest of Mt. Ruapehu) showed the same features for both regions. Therefore, we attribute our observations to disturbances in geomagnetic activity rather than to electromagnetic bursts or other possible earthquake precursors. Significantly lower coherences as compared to the Australian data are related to the generally higher noise level on the volcano, which is a popular recreation area, and to the lack of a more remotely located reference site for more effective removal of local noise.

Our investigations of MT transfer functions at Mt. Ruapehu do not show any obvious sudden changes that can be related to the two largest earthquakes that occurred during the 6 week duration of the MT measurements. The lack of any discernible trend also suggests that no gradual changes in conductivity structure occurred over the (possibly too short) 6 week duration of our measurements.

Andes

The data for this study were collected during four campaigns conducted along profiles extending across the Cordillera chain from the Pacific Ocean to the Antiplano between 1993 and 1998 (Brasse *et al.* 2002). The coordinates and recording durations of the MT sites were compared with the epicentres and occurrence times of large earthquakes taken from the CNSS (Council of the National Seismic System, http://quake.geo.berkeley.edu/cnss/) earthquake database. The nearest large magnitude earthquake in the available data set was an M4.4 earthquake that occurred, on 1999 January 9, approximately 30 km from site QGA located in the western Cordillera in northern Chile (Fig. 7). The focal depth of this earthquake was approximately 100 km. Soyer (2002) modelled an average bulk resistivity of ∼100–200 Ωm for this region. Thus MT transfer functions

© 2006 The Authors, *GJI*, **165,** 763–774
Journal compilation © 2006 RAS

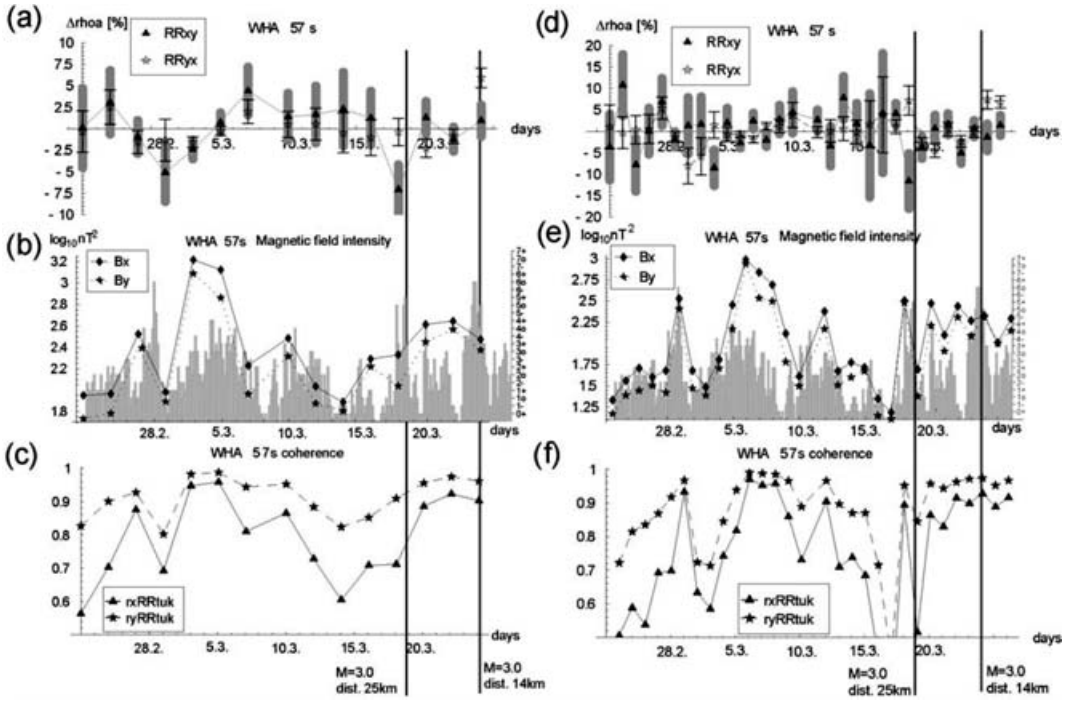

Figure 6. (a) Temporal variations of the apparent resistivity (as deviations from expected values) (b) magnetic field intensities and (c) coherences at site WHA (RR site TUK), New Zealand, derived from 48-hr-processing intervals for a period of 57 s. (d–f) show the same graphs for intervals of 24 hr length. Data points are plotted at the beginning of each interval, and error bars indicate 68 per cent confidence intervals. The vertical lines indicate the times at which the two largest earthquakes highlighted in Fig. 2 occurred.

from a period of ∼350 s should be most sensitive to the focal depth, and their horizontal adjustment length (Ranganayaki & Madden 1980) should exceed 30 km. The 30 day time-series from site QGA was divided into 48 hr intervals that were independently processed. Site CTE ∼110 km to the southwest (Fig. 7) was used as the remote reference station while sites CTE and GER were used for the MS processing. Fig. 8 shows results from SS, RR and MS processing for the apparent resistivities magnetic field intensities and coherences. Impedance phases and ssq values show temporal behaviours similar to the variations in apparent resistivities and are, therefore, not shown.

Two components of the apparent resistivities obtained from SS, RR and MS processing are plotted in Figs 8(a) and (b). Their comparison reveals variations of up to 10 per cent in *xy* (N–S direction)

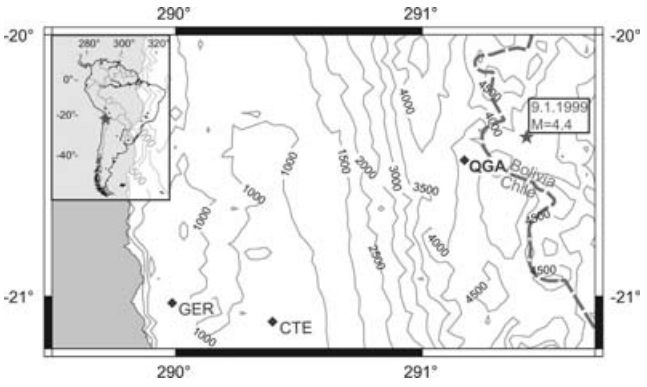

Figure 7. Topographic map of the area around site QGA in the Chilean Andes. The epicentre of a M4.4 earthquake that occurred on 1999 January 9 and the locations of sites used for RR processing are shown.

while variations in *yx* (E–W) are below 4 per cent. The different resolutions for the two components originates in current channelling effects at site QGA. These occur when narrow elongated conductive structures lead to very small electric fields along the strike resulting in reduced signal-to-noise ratios and, therefore, larger error levels and transfer function variations for that component. Evidence for channelling effects can be obtained from rotational analysis of the MT transfer functions (e.g. Bahr 1991). Current channelling leads to a strong rotational dependence of the apparent resistivities, phases and skew angles rendering their stability and error levels strongly coordinate-system dependent. Due to large amplitude differences between the elements of the impedance tensor in the presence of current channelling, amplitude-dependent rotational invariants such as ssq are dominated by the high-amplitude component.

Similar to the previous examples, the SS *xy* apparent resistivities show rather large variations and are down-biased for nearly all intervals. This effect does not appear in the RR- and MS-processed data. This could be for one of two reasons (i) violations of the PWA due to disturbances in the Earth's magnetosphere, (ii) non-stationary magnetic fields due to an earthquake precursor at QGA, which have a shorter correlation length than the distance between QGA and GER. Most of the largest deviations from apparent resistivity mean values coincide with intervals of low coherence. At day 14, strong deviations in SS processed results occur even though the observed magnetic field amplitudes are high. Examination of the magnetic field time-series of all available sites (not plotted) revealed disturbed daily variations during this time. Such source field complexities may lead to a violation of the PWA on which the estimation of the MT transfer functions is founded. Under these circumstances, the coherence length of the magnetic noise may be larger than the separation between local (QGA) and remote (GER, CTE) sites and the errors in transfer functions may be underestimated. Hence we attribute the

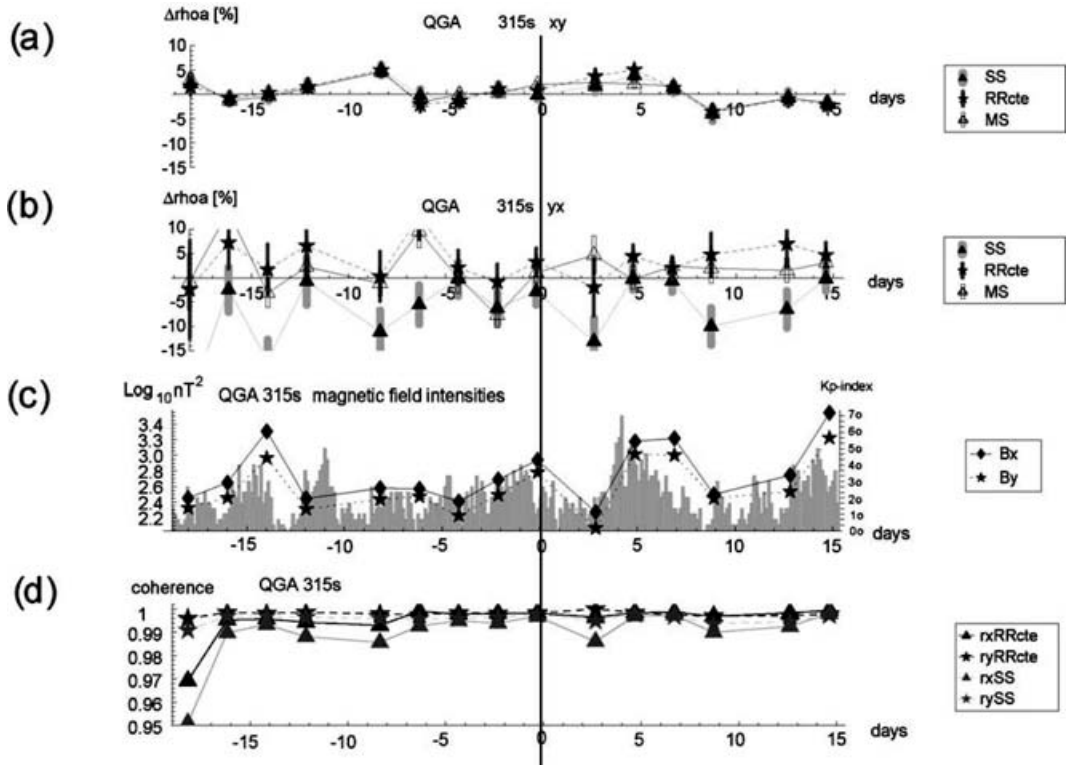

Figure 8. Temporal variations of (a) the apparent resistivity (deviations from expected values) for N–S, (b) and E–W directions, (c) the horizontal magnetic field intensities and (d) the coherences at a period of 315 s for site QGA in the Andes. Each data point represents a 48 hr interval. The penetration depth of this period is similar to the epicentral depth of an earthquake that occurred on day 0 of the timescale, at a distance of 30 km from site QGA. Site CTE was used as the remote reference and sites CTE and GER for the MS processing. The grey bars in (c) indicate the 3-hourly, geomagnetic kp-index for the recording interval (data from ftp.gfz-potsdam.de/pub/home/obs/kp-ap/).

apparent temporal variations in the apparent resistivities to noise in the external source field. We expect that non-stationary disturbances of the external magnetic field will often limit our ability to unequivocally distinguish electromagnetic precursors using passive electromagnetic methods.

Island of Montecristo

In 1997 late September and early October, a series of earthquakes (including the M5.9 Assisi earthquake of September 26) occurred on the central Italian mainland. During this time interval, continuous recording of MT data was being performed at two MT stations installed ∼500 m apart on the Mediterranean island of Montecristo, located west of the Italian coastline, for the purpose of studying mantle conductivity (Simpson 2002a). On October 6th, approximately 9 hr before an M5.7 earthquake occurred in central Italy the electromagnetic time-series recorded at the two island MT stations are characterized by sudden offsets in electric and magnetic field components. At this time, the island was uninhabited. In the absence of a physical model to explain how electromagnetic precursors could possibly be detectable at distances of ∼200 km from the epicentre, it seems likely that the sudden offsets in the electromagnetic time-series occurred in response to a local disturbance rather than as a direct precursor of the earthquake that occurred on the mainland. That a seismic disturbance had occurred on the island was evident when the instruments were serviced at a later date, and the heads of the fluxgate magnetometers were noted to have shifted their orientations. The sizes of the offsets (of order 100 nT) in the magnetic fields were consistent with the degree of reorientation (half a degree horizontal rotation, 0.2 degree tilt) of the magnetometers, and were hence attributed to seismic rather than to electromagnetic phenomena (Simpson 2002b). Changes in apparent resistivity immediately anteceding the presumed seismic disturbance were observed, but Simpson (2002b) attributed these to low coherence between electric and magnetic field components during this time. In 1997 November, the apparent resistivities were found to be the same as those in July of the same year (Simpson 2002b).

Application of our method to 3 day intervals of these data revealed the apparent resistivities to be relatively stable with the exception of the interval containing the offset (on 1997 October 5) and perturbations centred around 1997 October 16 and 1997 October 28, which have large confidence intervals (Fig. 9). During all of these intervals geomagnetic activity was very low (Fig. 9) and, as suggested by Simpson (2002b), low signal-to-noise may explain the down-biasing of the MT transfer functions. The generally stronger variations in the apparent resistivities compared to the previous examples are due to a high noise level in the data and the lack of a suitably located site for remote reference, both local and remote sites being influenced by storms and tides in the Mediterranean.

6 CONCLUSIONS

The confidence intervals obtained for MT transfer functions are a function of the number of independent estimates that are stacked in order to obtain them. Hence MT transfer functions with confidence intervals <1 per cent can be routinely obtained from electromagnetic data recorded for the purpose of probing the (presumed temporarily constant) conductivity structure of the Earth by deploying

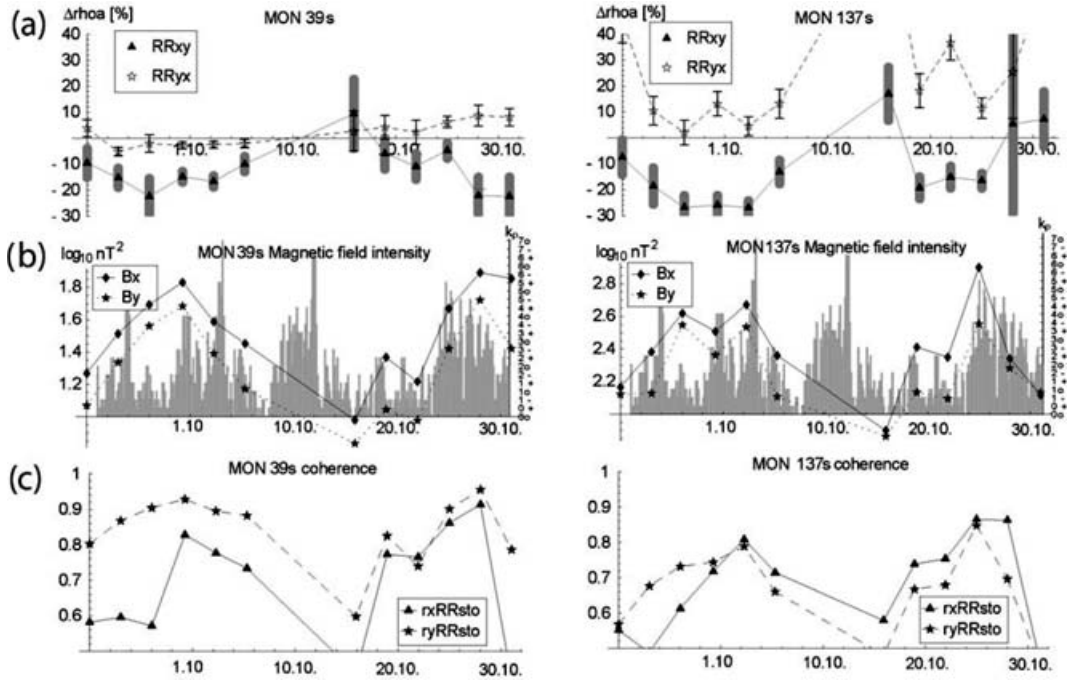

Figure 9. Temporal variations of the apparent resistivity (deviations from mean values) and horizontal magnetic field intensities for periods of 64 and 128 s at site 'MON' on Montecristo. Each data point is centred on a 3 day time interval. A gap in the recording occurred from 1997 October 7 to 1997 October 14. The grey bars show the 3 hr, geomagnetic kp-index for the same time interval (data from ftp.gfz-potsdam.de/pub/home/obs/kp-ap/).

instruments for appropriate recording durations and using appropriate processing techniques. On the other hand, in attempting to identify earthquake precursors, the length of time-series used to compute the MT transfer function will often be less than ideal for minimizing extraneous noise. In the examples presented, variations of ∼3 per cent (for periods around 100 s and 24–48 hr intervals) were observed in the apparent resistivities. Deviations usually occurred during times of low or disturbed geomagnetic activity. Larger apparent resistivity variations should be resolvable with the MT method but could not be found in the data sets studied. Time intervals not exceeding 24 hr are required in order to achieve the above mentioned stability. On the other hand variations of less then 1 per cent can be achieved if intervals of a couple of weeks are used in order to investigate long term trends. Ultimately, the resolution depends on the local noise levels, the geomagnetic activity during the measurements and the conductivity structure below the site. At present, the timescale over which changes in subsurface conductivity (if any) occur prior to an earthquake is uncertain.

In considering a possible role for the MT method in earthquake monitoring it is necessary to distinguish between two possible phenomena, the data processing requirements for the detection of which will in general be mutually exclusive:

(i) non-stationary electromagnetic disturbances of the source field and

(ii) long-term changes in the Earth's electrical conductivity

Whereas the improved stability of the transfer functions obtainable with RR or MS processing should enhance the chances of detecting (ii), MS processing is designed to negate (i). RR or MS processing reduces the influence of sensor noise and localized source field effects on MT transfer functions obtained from short time intervals. However, these processing techniques may lead to any locally-occurring electromagnetic precursors also being identified as noise and filtered out. At the other extreme, visual inspections of electric or magnetic time-series from single station recordings, on which numerous claims relating to the detection of electromagnetic precursors made in the geophysical literature (see for example references in Bernard 1992) have been founded lack objectivity.

If the PWA used in the MT method is violated (as can well be expected when the Earth's external magnetic field is disturbed, or if non-stationary internal fields are generated by earthquake precursors) this will not be reflected in the error bars, which reflect only measurement errors and not violations in the assumptions of the chosen method. Hence we conclude that the MT method is not well suited for the problem of investigating earthquake precursors unless they are accompanied by changes in the Earth's conductivity structure.

The data sets analysed in this study have originally been recorded for the purpose of investigating local and regional structures rather than temporal changes in the conductivity of the subsurface. Therefore, recording times and site locations were not ideal. Field measurements specifically designed to investigate changes in the conductivity structure could improve the chance to resolve changes in subsurface conductivity. Long-term array measurements with small site spacings would be ideal for that purpose as they would:

(i) increase the chance to measure close to earthquake epicentres

(ii) allow MS processing of the data to improve the temporal resolution

(iii) provide sufficient data for thorough sensitivity investigations for each site

(iv) allow observations of long-term stabilities of the resistivities and

(v) provide data to produce a model of the regional conductivity structure of the subsurface.

ACKNOWLEDGMENTS

Collection of the data analysed in this paper was made possible by funding from Geophysics Institute, University of Göttingen (data from central Australia), Institute of Geological and Nuclear Sciences Innovation Award (Ruapehu data), and German Science Foundation grants (SFB 267 (Andes data) and Ba889/6-1 (Montecristo data)). Thanks to H. Brasse and W. Soyer for providing the data set from the Andes and for their helpful comments, and to G. Egbert for providing his processing code. We also thank Karsten Bahr, Alexander Gatzemeier, Paolo del Lama, Jörg Leibecker, Domenico di Mauro, Edgar Schneider and Jürgen Waterman for help with fieldwork. M. Everett, M. Unsworth and two anonymous reviewers made helpful comments on a previous version of this paper.

REFERENCES

Bahr, K., 1988. Interpretation of the magnetotelluric impedance tensor: regional induction and local telluric distortion, *J. Geophys.,* **62,** 119–127.

Bahr, K., 1991. Geological noise in magnetotelluric data: a classification of distortion types, *Phys. Earth planet. Inter.,* **66,** 24–38.

Bahr, K., 2000. Percolation in the crust derived from distortion of electric fields, *Geophys. Res. Lett.,* **27,** 1049–1052.

Bernabe, Y., 1998. Streaming potential in heterogeneous networks, *J. geophys. Res.,* **103,** 20 827–20 841.

Bernard, P., 1992. Plausibility of long distance electrotelluric precursors to earthquakes, *J. geophys. Res.,* **97,** 17 531–17 546.

Bolt, B.A., 1978. Incomplete formulations of the regression of earthquake magnitude with surface fault rupture length, *Geology,* **6**(4), 233–235.

Brasse, H., Lezaeta, P., Schwalenberg, K., Soyer, W. & Haak, V., 2002. The Bolivian Altiplano conductivity anomaly, *J. geophys. Res.,* **107**(5), EPM 4 (1–15).

Cagniard, L., 1953. Basic theory of the magneto-telluric method of geophysical prospecting, *Geophysics,* **18,** 605–635.

Egbert, G. & Booker, J.R., 1986. Robust estimation of geomagnetic transfer functions, *Geophys. J. R. astr. Soc.,* **87,** 173–194.

Egbert, G.D., 1997. Robust multiple-station magnetotelluric data processing, *Geophys. J. Int.,* **130,** 475–496.

Egbert, G.D., Eisel, M., Sierra Boyd, O. & Morrison, H.F., 2000. DC trains and Pc2s: Source effects in mid-latitude geomagnetic transfer functions, *Geophys. Res. Lett.,* **27,** 25–28.

Egbert, G., 2002. On the generation of ULF magnetic variations by conductivity fluctuations in a fault zone, *Pure appl. Geophys.,* **159,** 1205–1227.

Eisel, M. & Egbert, G., 2001. On the stability of magnetotelluric transfer function estimates and the reliability of their variances, *Geophys. J. Int.,* **144,** 65–82.

Fraser-Smith, A., Bernardi, A., McGill, P., Ladd, M., Helliwell, R. & Villard, O., 1990. Low frequency magnetic field measurements near the epicentre of the Ms 7.1 Loma Prieta Earthquake, *Geophys. Res. Lett.,* **17,** 1465–1468.

Gamble, J., Wood, C., Price, R., Smith, I., Stewart, R. & Waight, T., 1999. A fifty year perspective of magmatic evolution on Ruapehu volcano, New Zealand: verification of open system behaviour in an arc volcano, *Earth planet. Sci. Lett.,* **170,** 301–314.

Gamble, T.D., Goubau, W.M. & Clarke, J., 1979. Error analysis for remote reference magnetotellurics, *Geophysics,* **44,** 959–968.

Gueguen, Y., David, C. & Gavrilenko, P., 1991. Percolation networks and fluid transport in the crust, *Geophys. Res. Lett.,* **18,** 931–934.

Hautot, S., 2005. Modeling temporal variations of electrical resistivity associated with pore pressure change in a kilometer-scale natural system, *Geochem. Geophys. Geosyst.,* **6,** doi:10.1029/2004GC000859.

Hayakawa, M., Kawate, R., Molchanov, O. & Yumoto, K., 1996. Results of ultra-low frequency magnetic field measurements during the Guam earthquake of 8 August 1993, *Geophys. Res. Lett.,* **23,** 241–244.

Honkura, Y. & Kuwata, Y., 1993. Estimation of electric fields in the conducting earth's crust for oscillating electric current dipole sources and implications for anomalous electric fields associated with earthquakes, *Tectonophysics,* **224,** 257–263.

Johnston, M., 1997. Review of electric and magnetic fields accompanying seismic and volcanic activity, *Surv. Geophys.,* **18,** 441–475.

Mackie, R.L. & Booker, J.R., 1999. Documentation for mtd3fwd and d3_to_mt. GSY-USA, Inc., 2261 Market St., Suite 643, San Francisco, CA 94114, user documentation.

Madden, T.R., LaTorraca, G.A. & Park, S.K., 1993. Electrical conductivity variations around the Palmdale section of the San Andreas fault zone, *J. geophys. Res.,* **98,** 795–808.

Merzer, M. & Klemperer, S., 1997. Modeling low-frequency magnetic-field precursors to the Loma Prieta earthquake with a precursory increase in fault-zone conductivity, *Pure appl. Geophys.,* **150,** 217–248.

Molchanov, O., Kopytenko, Y., Voronov, P., Kopytenko, E., Matiashvili, T., Fraser-Smith, A. & Bernardi, A., 1992. Results of ULF magnetic field measurements near the epicenters of the Spitak (Ms = 6.9) and Loma Prieta (Ms = 7.1) earthquakes: comparative analysis, *Geophys. Res. Lett.,* **19,** 1495–1498.

Park, S.K., 1991. Monitoring resistivity changes prior to earthquakes in Parkfield, California, with telluric arrays, *J. geophys. Res.,* **96,** 14 211–14 237.

Park, S., Johnston, M.J.S., Madden, T. & Morrison, H.F., 1993. Electromagnetic precursors to earthquakes in the ULF band: A review of observations and mechanisms, *Rev. Geophys.,* **31,** 117–132.

Ranganayaki, R.P. & Madden, T.R., 1980. Generalized thin sheet analysis in magnetotellurics: An extension of Price's Analysis, *Geophys. J. R. astr. Soc.,* **60,** 445–457.

Rangarajan, G.K., 1989. Indices of geomagnetic activity, in *Geomagnetism*, **Vol. 3,** pp. 323-384, ed. Jacobs, J.A., Academic Press, London.

Roberts, J., Duba, A., Mathez, E., Shankland, T. & Kinzler, R., 1999. Carbon-enhanced electrical conductivity during fracture of rocks, *J. geophys. Res.,* **104,** 737–747.

Sasai, Y., Uyeshima, M., Zlotnicki, J., Utada, H., Kagiyama, T., Hashimoto, T. & Takahashi, Y., 2002. Magnetic and electric observations during the 2000 activity of Miyake-Jima volcano, central Japan, *Earth planet. Sci. Lett.,* **203,** 769–777.

Simpson, F., 2001. Resistance to mantle flow inferred from the electromagnetic strike of the Australian upper mantle, *Nature,* **412,** 632–635.

Simpson, F., 2002a. A comparison of electromagnetic distortion and resolution of upper mantle conductivities beneath continental Europe and the Mediterranean using islands as windows, *Phys. Earth planet. Inter.,* **129,** 117–130.

Simpson, F., 2002b. Stress, stress release and geoelectromagnetism, in *Seismotectonics in Convergent Plate Boundary*, eds Fujinawa, Y. & Yoshida, A., Terra Scientific Publishing Company, Tokyo.

Simpson, F. & Bahr, K., 2005. *Practical magnetotellurics*, Cambridge University Press, p. 272

Sims, W., Bostick, F., Smith, H., 1971. The estimation of magnetotelluric impedance tensor elements from measured data, *Geophysics,* **36,** 938–942.

Soyer, W., 2002. Analysis of geomagnetic variations in the central and southern Andes, *PhD thesis,* Freie Universität Berlin.

Steveling, E. & Leven, M., 1992. Ein Datenlogger für niederfrequente geophysikalische Messungen., 14. Kolloquium zur elektromagnetischen Tiefenforschung in Borkheide vom 25-29.5.1992. Deutsche Geophysikalische Gesellschaft (in German).

Szarka, L. & Menvielle, M., 1997. Analysis of rotational invariants of the magnetotelluric impedance tensor, *Geophys. J. Int.,* **129,** 133–142.

Unsworth, M. & Bedrosian, P.A., 2004. Electrical resistivity structure at the SAFOD site from magnetotelluric exploration, *Geophys. Res. Lett.,* **31,** doi:10.1029/2003GL019405.

Yoshida, S., Clint, O.C. & Sammonds, P., 1998. Electric potential changes prior to shear fracture in dry and saturated rocks, *Geophys. Res. Lett.,* **25,** 1577–1580.

Zlotnicki, J. & Le Mouel, J., 1990. Possible electrokinetic origin of large magnetic variations at la Fournaise volcano, *Nature,* **343,** 633–636.

Zlotnicki, J. et al., 2003. Resistivity and self-potential changes associated with volcanic activity: the July 8,2000 Miyake-Jima eruption (Japan), *Earth planet. Sci. Lett.,* **205,** 139–154.

© 2006 The Authors, *GJI*, **165,** 763–774
Journal compilation © 2006 RAS